Atomic Resolution Imaging of the Edges of Catalytically Etched Suspended Few-Layer Graphene

Franziska Schäffel,[†,*] Mark Wilson,[‡] Alicja Bachmatiuk,[§] Mark H. Rümmeli,[§,⊥] Ute Queitsch,[§] Bernd Rellinghaus,[§] G. Andrew D. Briggs,[†] and Jamie H. Warner[†]

[†]Department of Materials, University of Oxford, Parks Road, Oxford OX1 3PH, United Kingdom, [‡]Department of Chemistry, University of Oxford, South Parks Road, Oxford OX1 3QZ, United Kingdom, [§]IFW Dresden, P.O. Box 270116, D-01171 Dresden, Germany, and [⊥]University of Technology Dresden, 01062 Dresden, Germany

ABSTRACT Nanostructured graphene and graphene nanoribbons have been fabricated by catalytic hydrogenation, and the edge smoothness has been examined *via* direct imaging with atomic resolution. When abstaining from solvents during sample preparation, the prepared nanoribbons possess clean edges ready for inspection *via* transmission electron microscopy (TEM). Edges with subnanometer smoothness could be observed. A method has been developed to make catalytic hydrogenation experiments compatible with TEM, which enables monitoring of the nanoparticles prior to and after hydrogenation. In this way, etching of free-standing few-layer graphene could be demonstrated. Our results enable evaluation of the degree of edge control that can be achieved by means of catalytic hydrogenation.

KEYWORDS: nanofabrication · graphene nanoribbons · catalytic hydrogenation · edge smoothness · low voltage transmission electron microscopy

Given its fairly recent experimental discovery in 2004,[1] research on graphene has become a major field of nanoscience and created very strong interdisciplinary interest, due to graphene's exceptional properties. Besides its high strength and stiffness, which make graphene highly appealing for application in composite materials, strong effort goes into pushing forward nanoelectronic applications due to the observation of near-ballistic transport at room temperature, extremely high intrinsic carrier mobilities, and superb thermal conductivity.[2−6] Owing to the fact that truly two-dimensional graphene is a semimetal, it needs to be processed into graphene nanoribbons (GNRs) in order to open a band gap and thus accomplish its integration in semiconducting nanoelectronics.[7,8] To take advantage of graphene's extreme properties, it is imperative that the edges of such nanostructured graphenes are crystallographically well-defined and, ideally, atomically smooth to reduce the negative impact of edges on electrical and thermal conduction properties *via* scattering of electrons and acoustic phonons on the edges.[6,9−12]

Graphene edges have been widely studied using (high-resolution) transmission electron microscopy ((HR)-TEM),[13−16] scanning tunneling microscopy (STM),[17−20] and Raman spectroscopy.[21,22] However, not many studies can be found in literature on the edges of *structured* graphenes. Here, quality control is mainly based on Raman spectroscopy.[23] Also low-magnification microscopy—for example, atomic force microscopy (AFM) or scanning electron microscopy (SEM)—has been carried out, which may show smooth edges on a microscopic scale, but has not yet revealed the edge smoothness at the atomic level.[24−26]

A variety of methods have been introduced to structure graphene, including electron beam lithography,[7,8] scanning tunneling microscope lithography,[27] sonochemical methods,[24,28] carbo-thermal reduction of SiO_2,[29] and *bottom-up* growth.[30,31] GNRs have also been reported from unzipping carbon nanotubes (CNTs) by various methods.[32−35] However, the process conditions applied may affect the structure of the GNRs in a way, inducing defects instead of just opening up the CNT.[32−34] The reported *top-down* approaches have not yet demonstrated control at the atomic level, with the possible exceptions of the sonochemical method[24] and the carbo-thermal reduction of SiO_2,[29] where quality control with Raman spectroscopy[22,29] was indicative of smooth zigzag edges. However, direct imaging of the atomic structure and knowledge of the smoothness of the edges on the atomic level has yet to be fully realized.

* Address correspondence to franziska.schaeffel@materials.ox.ac.uk.

Received for review November 9, 2010 and accepted January 27, 2011.

Published online February 23, 2011
10.1021/nn103035y

Recently, catalytic etching of graphite or graphene by metallic and nonmetallic nanoparticles has been considered to be a key technology for the fabrication of graphene nanostructures and the tailoring of GNRs.[25,26,36−39] In brief, when exposed to hydrogen under elevated temperatures, the nanoparticles act as knives and cut through the carbon they are in contact with, leaving pronounced etch tracks along specific crystallographic directions. It is this *intrinsic crystallographic etching* that is the reason for the popularity of catalytic hydrogenation methods in graphene nanostructuring. Thorough characterization and evaluation of the atomic structure of the nanoribbon edges with imaging techniques has, however, not yet been accomplished.

Here, we report on catalytic hydrogenation experiments catalyzed by gas-phase-prepared cobalt nanoparticles. We successfully processed nanostructured graphenes and GNRs with clean edges ready for inspection using low voltage HRTEM (LV-HRTEM). In this way, edges with subnanometer smoothness could be observed. Further, a method has been developed to make catalytic hydrogenation experiments compatible with TEM, and thus, the experimental steps of catalytic hydrogenation could be monitored throughout the process and the etching of free-standing few-layer graphene (FLG) could be demonstrated. These results allow us to evaluate the degree of edge control that can be achieved by catalytic hydrogenation.

RESULTS AND DISCUSSION

In order to find the best possible etching conditions and suitable starting materials, we have investigated different types of catalyst particles as well as different graphite precursors under various process temperatures. The respective results, together with TEM micrographs, are summarized in the Supporting Information. They led to the conclusion that the best results with regard to the formation of microscopically straight edge patterns are obtained using highly oriented pyrolytic graphite (HOPG) as graphite precursor in combination with gas-phase-prepared Co nanoparticles. With the general aim of this work in mind, that is, the evaluation of edge smoothness obtained from catalytic hydrogenation, "bulk" catalytic hydrogenation experiments (namely, experiments that are *not* directly carried out on a TEM grid but on larger Si chips) pointed to another obstacle that needed to be addressed. In the process of examining the catalytically etched samples, carbonaceous residue, especially at freshly etched graphene edges, often hindered proper characterization of the actual edge structure. This is not surprising since the catalytic etching process essentially creates highly reactive dangling bonds that will react with any debris in close vicinity. If a cleaner graphene flake was produced, the hydrogen present in the hydrogenation reaction may saturate the dangling bonds instead, leaving a cleaner edge.

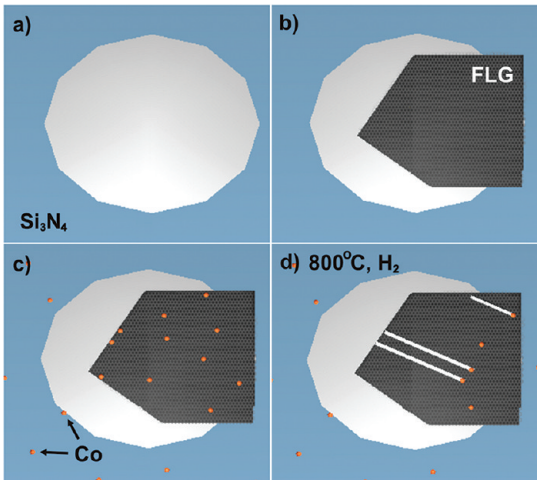

Figure 1. Schematic of sample preparation: (a) perforated Si_3N_4 TEM membrane grid; (b) FLG as deposited from methanol solution and spanned across the hole in the Si_3N_4 membrane; (c) deposition of catalyst particles (Co nanoparticles); (d) anisotropic etch track formation in H_2 atmosphere at elevated temperatures through particles residing close to a graphene edge.

Therefore, in our experiments fabricating few-layer graphenes, we concentrated on producing graphenes with as little carbonaceous residue attached to them as possible. In general, using solvents (especially ones with a high boiling point) increases the amount of debris. Hence, using gas-phase-prepared catalyst particles instead of wet chemically prepared particles is one step toward cleaner edges. Further, typical solvents for graphite liquid phase exfoliation (*e.g.*, *N*-methylpyrrolidone) have a high boiling point ($T_B \sim$ 203 °C) which intrinsically yields graphenes covered with residual species.[40] We therefore prepared mechanically exfoliated graphene from HOPG flakes by simply crushing a HOPG flake with mortar and pestle and collected the smaller pieces with methanol (T_B = 64.7 °C) which is much more volatile. This procedure yields TEM transparent graphite sheets as well as a significant amount of FLG sheets consisting of approximately 5−10 layers of graphene (see Supporting Information for layer number determination).

The schematics in Figure 1 summarize the sample preparation steps. Perforated Si_3N_4 membrane TEM grids (Figure 1a) can easily withstand a high-temperature treatment, and contamination stemming from the grid during such experiments can be neglected (as opposed to heating standard TEM mesh grids which are coated with a perforated amorphous carbon film). Therefore, this approach enables one to monitor the different experimental steps of catalytic hydrogenation as schematically highlighted in Figure 1b−d. Figure 1b depicts a pristine FLG flake as deposited from the methanol solution and suspended across the hole in the Si_3N_4 membrane. Catalytic hydrogenation

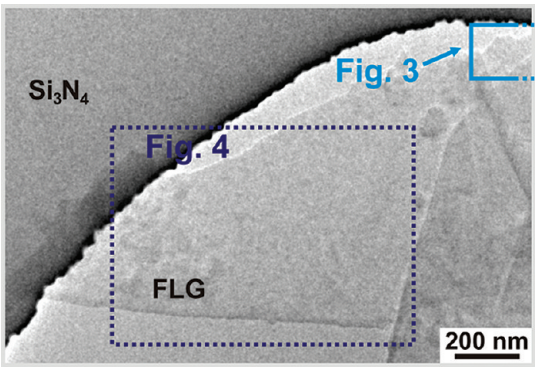

Figure 2. Suspended FLG flake as derived from placing a few drops of the methanol solution onto a perforated Si_3N_4 TEM membrane grid. The areas marked with squares are the ones examined in more detail and presented in Figures 3 and 4.

requires a catalyst. In our experiment, catalytic Co nanoparticles are deposited from the gas phase and randomly land on the FLG flake as well as the Si_3N_4 membrane (Figure 1c). Upon exposure to hydrogen at elevated temperature, particles that are placed close to a graphene edge then act as knives and anisotropically etch the FLG flake (Figure 1d).

As an example, Figure 2 shows a TEM micrograph of a pristine FLG flake as derived from placing a few drops of the graphene containing methanol solution onto a perforated Si_3N_4 TEM grid. The colored boxes in Figure 2 represent the sample areas that have been investigated in greater detail and are presented in Figures 3 and 4.

Figure 3a shows the section marked light blue in the flake in Figure 2 after deposition of gas-phase-prepared Co nanoparticles. The isolated catalyst particles have a mean diameter of 7.6 nm and are randomly spread over the FLG flake. A graphene step edge can be observed in the image, and some particles—marked with red circles—are placed at this step edge or in close vicinity, which is interesting in that catalytic etching usually commences at an exposed graphite or graphene edge due to interaction with the dangling bonds at that edge. Figure 3b shows the same flake section after exposing the sample to hydrogen at 800 °C for 1 h. Clearly four etch tracks, starting from the step edge, have evolved during the hydrogen treatment. The particle positions in Figure 3a correlate with the etch track starting points as highlighted by the dotted red circles in Figure 3b, indicating that the particle has to find an edge in order to initiate the lateral process of etching. Three pronounced tracks go along the same crystallographic direction forming two nanoribbons, supported by graphene, with widths of roughly 5 and 11 nm. The particle residing within the middle track (track 2) most probably formed through coalescence of surrounding particles (marked with white arrows in Figure 3a) after track formation. A fourth track at the bottom right of the image exhibits an etch direction which differs by 60° with respect to the other three tracks. This indicates that the etch tracks are commensurate with the graphite lattice.

Analysis of the fast Fourier transformations (FFTs) of high-resolution TEM images reveals that in these experiments etching preferentially occurs along the $\langle 11\bar{2}0\rangle$ directions, the so-called zigzag directions, ideally leaving zigzag edges behind. Figure 3c presents a high-resolution TEM micrograph of the section marked orange in Figure 3b (rotated clockwise by 50°). Figure 3d,e depicts FFT-enhanced high-resolution TEM micrographs of the areas marked yellow and green in Figure 3c, respectively, together with their FFTs as insets. The FFT of the area marked yellow (inset in Figure 3d) reveals the crystal orientation of the "underlying" graphene layers, that is, the layers which have apparently supported the particles during the catalytic hydrogenation process. The six FFT reflexes marked with yellow circles arise from the $\{10\bar{1}0\}$ lattice planes, indicating the $\langle 10\bar{1}0\rangle$ armchair directions. In Figure 3e, a Moiré pattern becomes apparent, and in the corresponding FFT (inset in Figure 3e), a second set of six spots is observed—marked with green circles—which is rotated by 20° with respect to the first set of reflexes. Figure 3e and its FFT contain the crystallographic information of both the underlying graphene layers and the top layers forming the step edge. Both Moiré pattern and the rotation of the FFT spots are indicative of a rotational stacking fault.[41] The green arrows in the FFT represent the $\langle 11\bar{2}0\rangle$ zigzag directions within the top etched graphene layers, one of which coincides with the etching direction (green arrow in Figure 3c).

While the contrast of tracks 1 and 2 appears as bright as that of the underlying FLG sheet, the etch track located farthest to the right among the three adjacent tracks (track 3) in Figure 3b exhibits a less pronounced contrast, which indicates that the top graphene layers are only partly etched with respect to the underlying FLG sheet and the track is not as deep as in the two other cases (tracks 1 and 2). FFT analysis within track 3 also reveals both sets of FFT spots, indicating that the stacking fault lies somewhere within the graphene layers between underlying layers and the top layers etched by particle 3 (*cf.* Figure S3c in the Supporting Information). Most likely, it is placed at the interface between the underlying FLG sheet and the top FLG sheet that forms the actual step edge.

Another interesting result can be derived when taking into account the pristine particle sizes. While the deeper tracks 1 and 2 are formed by the smaller particles, the shallower track 3 is etched in a place where more catalyst material is available. Therefore, the common picture of the catalyst particle diameter simply determining the track width and depth should be revisited. Future *in situ* TEM studies on catalytic hydrogenation are mandatory in order to deeper

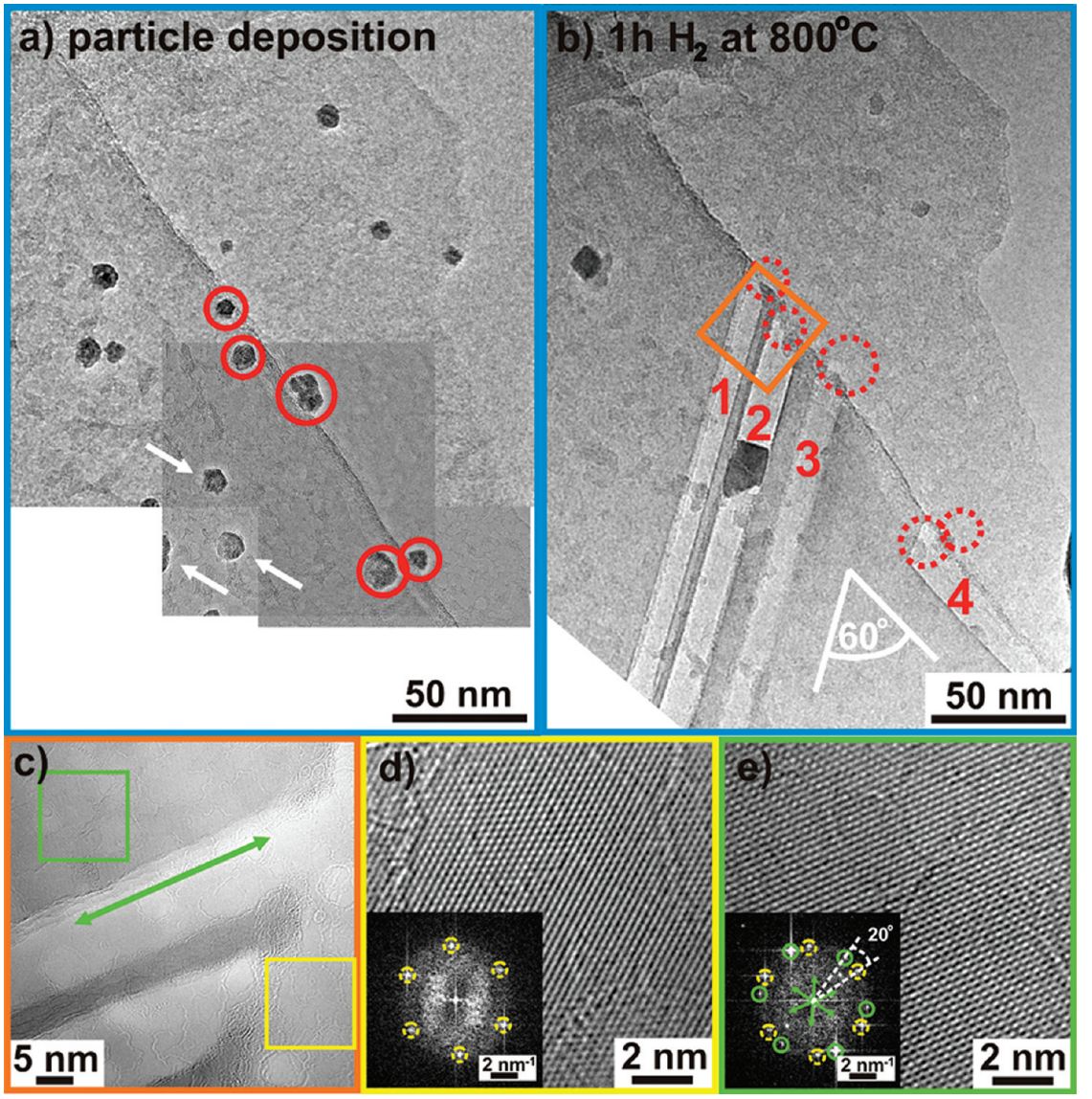

Figure 3. Use of robust perforated Si_3N_4 TEM grids enables one to monitor the different process steps of catalytic hydrogenation: (a) FLG flake after deposition of gas-phase-prepared Co nanoparticles; (b) FLG flake after catalytic hydrogenation at 800 °C for 1 h; (c) HRTEM micrograph of the area marked orange in panel b; the image is rotated clockwise by 50°; (d,e) FFT-enhanced HRTEM micrographs and their FFTs (as insets) of the areas marked yellow and green in panel c, respectively. All circles in the FFTs resemble armchair directions in the graphite lattice. In the FFT of panel e, two sets of armchair directions are observed, which is indicative of a rotational stacking fault. The green arrows in panel e resemble the graphite zigzag directions with respect to the green circled armchair spots, indicating that the etching direction is a zigzag direction.

understand and gain control over the underlying processes. Further, the present analysis also demonstrates that determining the etch direction from the underlying graphite may not always give a correct answer as rotational stacking faults have to be taken into account.

A second scenario that is observed investigating catalytic hydrogenation of suspended FLG is depicted in Figure 4. Figure 4a shows a section of the flake marked with a purple rectangle in figure 2 after deposition of gas-phase-prepared Co nanoparticles. This graphene sheet does not exhibit a step edge. Yet, some catalyst particles can be found close to the sheet edge some of which are highlighted with red circles. Remarkably, after catalytic hydrogenation at 800 °C for 1 h, some of these particles have formed straight etch tracks that go through all the layers of the FLG sheet (Figure 4b). The particles etching tracks remain attached to the graphene interface despite having no support beneath and do not drop through the sheet. Therefore *etching of free-standing FLG via catalytic hydrogenation* has been demonstrated for the first time.

Comparing Figure 4a,b, the appearance of the catalyst material changes notably. With a few exceptions, the catalyst particles have moved away from their original position even when they did not etch a track. Further, the catalyst particles in Figure 4b, especially

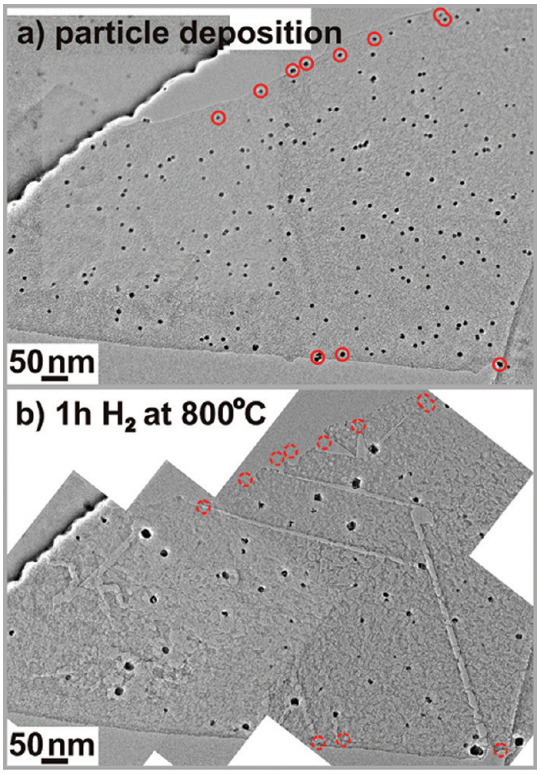

Figure 4. Catalytic etching of free-standing FLG: (a) FLG flake after deposition of gas-phase-prepared Co nanoparticles and (b) after catalytic hydrogenation at 800 °C for 1 h.

the ones that have etched tracks, have coalesced, now forming larger particles with a mean diameter of 10.8 nm and a much larger diameter distribution as compared to the pristine particles which had a mean diameter of 7.6 nm. This coalescence may be the reason for the zigzag direction being the preferred etching direction as opposed to previous reports, where small nanoparticles (Ni and Co) with diameters below 10 nm showed preferential etching along the armchair directions,[25,38] which has also been supported by kinetic Monte Carlo simulations.[25] Additionally, the number of catalyst particles is significantly reduced during the hydrogen treatment. However, quantitatively, the depletion of catalyst material, as derived from the total particle volume (assuming spherical particles) per unit area, before and after the hydrogen treatment only amounts to 8.2%.

In the lower left area of the flake, etching has occurred in a more irregular way. Straight etch tracks can only be observed over short distances, and the (coalesced) particles appear to have "mopped up" a surrounding area much rather than etched a track, as previously reported.[38] While in Figure 4a a fine coverage with an amorphous layer can be noticed, these amorphous species become more apparent in Figure 4b. Possibly the particles have pushed these species aside and, when loaded with too much matter, were deflected off their course. (Note that Figure 4b has been imaged after extensive HRTEM characterization. Despite the low accelerating voltage used in our TEM studies, the long exposure to the electron beam affects the sample, leading to atom displacement and roughening of the flake surface and graphene edges.)

The approach of using gas-phase-prepared catalyst nanoparticles in combination with graphenes prepared using a solvent with a low boiling point yields catalytically etched graphenes, where the edges are free of adsorbates and, as a result, are ready for characterization *via* HRTEM. It should be pointed out that the method of catalytic hydrogenation itself also provides easy distinction between folded and nonfolded graphene edges by simply tracing an etch track. Figure 5 presents HRTEM micrographs of typical graphene edges after catalytic hydrogenation. Figure S4 in the Supporting Information shows the corresponding overview TEM micrographs in which the investigated edges are marked with colored arrows, and the corresponding HRTEM micrographs and FFTs (Figure 5a−i) are framed with the respective color. The greater part of the edges appears to be free of residue as opposed to samples where wet chemically prepared catalyst particles were applied (*cf.* Figure S1e). This enables one to nonambiguously determine the edge roughness. For better clarity, the roughness measurement markers are not included in Figure 5 but are instead presented in Figure S5 in the Supporting Information, which also displays the marked areas from which the FFTs were determined.

The etch track in Figure 5a was formed by a particle that was still supported by underlying graphene layers. While the track appears to be straight on a microscopic level (Figure S4a), it reveals some discontinuity at the atomic scale. The bottom (green) edge is smooth at the left-hand side with a roughness of approximately 1.0 nm. Further to the right, the same edge appears to be bent slightly and the roughness increases to 1.5 nm (Figure S5a). In contrast to this, the top (blue) edge is terraced; that is, the top graphene layers seem to be etched more than the layers further down. The total roughness of the terraced edge amounts to ∼3 nm (Figure S5a), while each terrace itself exhibits a roughness which is comparable to the bottom edge (*i.e.*, ≤1.5 nm).

The edges presented in Figure 5c−i were formed *via* particles etching though the whole sheet of FLG, which were only attached to the sheet by the actual particle−carbon etch interface. It is even easier to determine the roughness of this type of etched graphene edge as compared to the previous case of etching with supported particles. Again, the edges appear to be free of residue. Along the same etch track, some graphene layers in the FLG sheet seem to be etched further than others (Figure 5c), however, in this case not in a terraced manner. Typically, the roughness is of the order of 1−2 nm (Figure S5), which is comparable to the values for the "green" edge as well as those for the terraces of the "blue" edge (Figure 5a). Further, edge

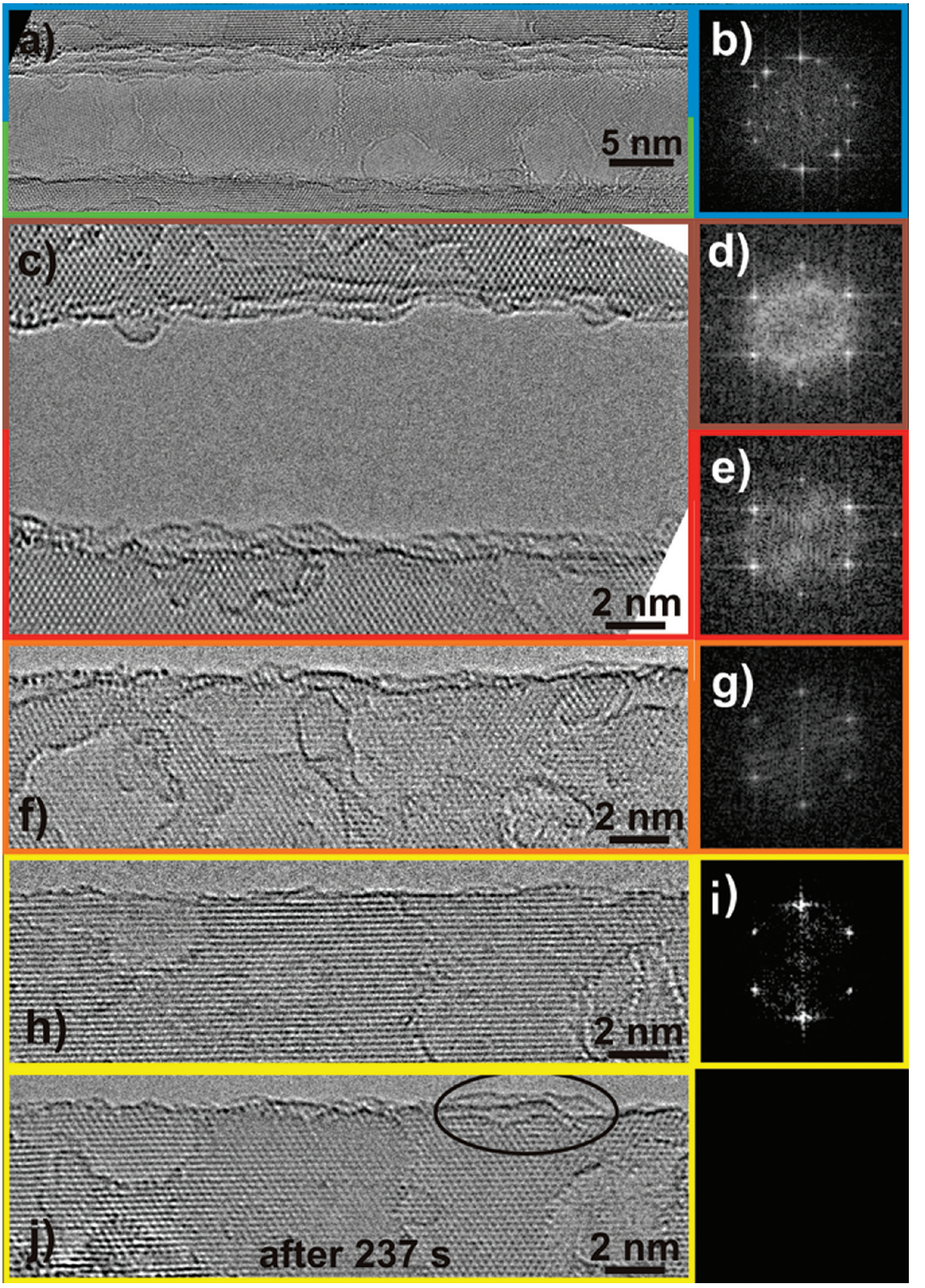

Figure 5. LV-HRTEM micrographs of etched graphene edges: (a) etch track with a smoother (bottom) and a terraced (top) edge formed from etching with a particle supported by underlying graphene layers and (b) corresponding FFT; (c−i) graphene edges as obtained from etching though all the layers of FLG and respective FFTs; (j) HRTEM micrograph of the same edge as in (h) after significant exposure to the electron beam. Due to the electron beam irradiation during HRTEM imaging, the sample is affected and the edge significantly roughens as compared to the pristine edge.

analysis also reveals that the edge roughness obtained is not regular. At the atomic scale, there are no oscillations detectable as, for example, in the case of previously observed sawtooth-type edges in extended

graphene sheets.[14] The edges do not seem to follow any patterning or faceting, not even on a short scale, and also do not show a preferential edge termination despite the *default* zigzag orientation of the etch track. The edges appear to be random, possibly because the moving particle re-deposits carbon at the edge that then may randomly rearrange itself.

Nevertheless, *subnanometer smoothness* can be obtained *via* catalytic hydrogenation. In the best case scenario of our present study (Figure 5h) a subnanometer edge smoothness of ~0.6 nm has been observed over an edge length above 25 nm. This smoothness value roughly compares to 4 times the carbon−carbon distance in graphite (a_{C-C} = 0.142 nm). Some shorter regions along this edge are nearly atomically smooth, which again highlights the potential of the catalytic hydrogenation process.

In order to determine reliable edge roughness values, it is imperative to take great care when interpreting the HRTEM micrographs. Figure 5j shows the same edge as Figure 5h after approximately 4 min of HRTEM imaging. The edge roughness has increased by 50% during this exposure to electron irradiation. Further, on the right-hand side of the edge, individual stacks of graphene layers have become apparent with strong lines of contrast (black ellipse). This also explains why we decided to carry out high-resolution edge characterization prior to taking overview micrographs. Clearly, the edge roughening as well as selective removal of monolayers in the FLG sheet by means of electron-beam-induced sputtering can be recognized in the overview in Figure S4b.[42]

In comparison, GNRs fabricated *via* STM lithography or *via* cutting carbon nanotubes using particles show edges that appear to be highly corrugated,[27,35,43] while some regions along the edges of our catalytically cut FLG sheets are nearly atomically smooth. Here studies on single-layer graphene together with in-depth structural edge characterization are needed to further substantiate the potential of the catalytic hydrogenation process. These results, however, demonstrate that HRTEM allows one to obtain much greater detail in observing the atomic edge structure as compared to previous studies using SEM, AFM, and STM which also predominantly focused on determining the edge orientation, not the actual edge morphology.[25,27] Following from this, GNRs fabricated *via* different approaches (*e.g.*, sonochemically or through etching with an Ar plasma) also have to be studied with high spatial resolution in order to be able to nonambiguously relate, for example, Raman measurements to the atomic edge structure.[22] So far, this was often hindered due to instrumentational reasons (*e.g.*, a too large AFM tip radius).[24]

CONCLUSION

We have fabricated nanostructured graphenes and GNRs *via* catalytic hydrogenation and examined the edge smoothness using LV-HRTEM. The amount of debris attached to freshly etched edges can be significantly reduced when abstaining from solvents during sample preparation, which is key to the fabrication of etched nanographenes with edges that are almost totally devoid of contamination and therefore allow for clear imaging and quantitative evaluation of their roughness. This enabled the first high-resolution study of the edges of nanostructured graphene using a direct imaging technique. Subnanometer edge smoothness has been obtained over a significant graphene edge length. Our studies also clearly highlight the benefits of using perforated Si_3N_4 TEM membrane grids for catalytic hydrogenation studies. In this way, we were able to monitor the nanoparticles prior to and after the hydrogenation step. We further observed two etching scenarios. In the first case, catalyst particle etches into the graphene sheets from a step edge while still being supported by underlying graphene layers. In the second case, we were able to demonstrate catalytic etching of free-standing FLG for the first time where the catalyst particles fully etch through all of the layers of the FLG sheet, having no support beneath. Further, the use of Si_3N_4 grids will not only allow for *in situ* hydrogenation studies on suspended graphene sheets but also opens up the possibility for future work on electronic characterization of nanostructured graphenes and subsequently facilitate the direct correlation of atomic edge structure and electronic properties.

METHODS

Highly oriented pyrolytic graphite (HOPG, from SPI supplies, SPI-2 grade) served as a precursor to mechanically exfoliate graphene. A larger HOPG flake was scratched off the HOPG block using a razor blade and crushed with mortar and pestle. Bigger HOPG pieces were removed with tweezers, while the smaller pieces were collected using methanol. For hydrogenation studies, a few drops of this methanol solution were placed onto a perforated Si_3N_4 TEM membrane grid (*cf.* Figure 1a,b). Si_3N_4 grids can withstand high process temperatures. Therefore, this approach allows for the preparation of samples where the graphene flakes can be examined prior to particle deposition and between particle deposition and the hydrogenation process, which is usually carried out at temperatures above 600 °C. TEM investigation always showed a mixture of thicker (but mainly TEM transparent) graphite pieces as well as a significant amount of few-layer graphene (FLG). This process of course is not designed to achieve high-yield graphene production. However, for the purpose of these studies, residual carbon resting on the FLG flakes, which may hinder proper TEM investigation of the graphene edges, was observed to be significantly less. Methanol is more volatile as compared to popular solvents used in liquid phase exfoliation. These solvents (*e.g.*, *N*-methylpyrrolidone) typically have a rather high boiling point and thus leave behind a lot of carbonaceous species on the FLG surface.[40,44]

Catalytic cobalt nanoparticles have been synthesized *via* inert gas condensation based on magnetron sputtering and simultaneously deposited onto the graphite precursor (Figure 1c) as well as a carbon-coated copper TEM reference grid.[45,46] The nanoparticles grow from a supersaturated metal vapor generated by dc sputtering from a cobalt target at a pressure of $p = 1.5$ mbar. The deposition time was 100 s. Upon sample transfer, these cobalt particles spontaneously oxidize.[47] When exposed to H_2 in the hydrogenation process, the particles are then reduced to metallic cobalt.[47]

Catalytic hydrogenation represents the decomposition (etching) of graphitic carbon in hydrogen atmosphere in the presence of a catalyst particle forming a hydrocarbon (CH_4) as reaction product (Figure 1d). We performed catalytic hydrogenation experiments in a horizontal CVD reactor equipped with a movable sample rod with an inner diameter of 23 mm. The Si_3N_4 grids were placed in an Al_2O_3 crucible and transferred into the sample rod. The oven was heated to 800 °C in Ar atmosphere. Once the temperature was reached, the gas atmosphere was switched to an Ar/H_2 gas mixture containing 25% H_2. The sample rod was then transferred into the hot oven zone and left for 1 h. The experiments were carried out at atmospheric pressure with a gas flow rate of 600 sccm. From scaled-up experiments, it is known that methane is the main reaction product.[36] Previous TEM studies further showed that the Co nanoparticles are in the metallic hexagonally close-packed phase during the hydrogenation process. During sample transfer, the particles appear to partly reoxidize. Carbide phases have not been detected in these studies.[38,47]

Conventional transmission electron microscopy of graphitic samples at standard accelerating voltages of 200 or 300 kV leads to sample destruction, which would make the investigation and evaluation of graphene edges difficult. At voltages below the so-called knock-on damage threshold for graphitic materials (*i.e.*, 86 kV),[48] conventional microscopes lack the resolution to atomically resolve the graphene lattice and the graphene edges. Only with the development of aberration correctors, atomic resolution imaging of carbon nanostructures, including graphene and its edges, became accessible.[13,14,49] Owing to graphene's pronounced susceptibility to radiation damage, structural and morphological investigations of the graphene edge were conducted using a JEOL JEM-4000EX TEM operated at 80 kV. High-resolution work was carried out using an image-corrected FEI Titan^3 80-300 microscope operated at 80 kV with beam current densities ≤ 0.1 pA·nm^{-2}.

Acknowledgment. F.S. and A.B. thank the Alexander von Humboldt foundation and the BMBF for their postdoctoral fellowships. F.S. also acknowledges funding from the EPSRC platform grant (EP/F048009/1). M.H.R. thanks the EU (ECEMP) and the Freistaat Sachsen. J.H.W. thanks the Royal Society, the Glasstone Fund, and Brasenose College for support.

Supporting Information Available: Bulk hydrogenation experiments determining the best process parameters. Details on the determination of the number of graphene layers. Detailed FFT analysis of the etched FLGs. Overview TEM micrographs. HRTEM micrographs including measurement markers for roughness evaluation. This material is available free of charge *via* the Internet at http://pubs.acs.org.

REFERENCES AND NOTES

1. Novoselov, K. S.; Geim, A. K.; Morozov, S. V.; Jiang, D.; Zhang, Y.; Dubonos, S. V.; Grigorieva, I. V.; Firsov, A. A. Electric Field Effect in Atomically Thin Carbon Films. *Science* **2004,** *306*, 666–669.
2. Lee, C.; Wei, X.; Kysar, J. W.; Hone, J. Measurement of the Elastic Properties and Intrinsic Strength of Monolayer Graphene. *Science* **2008,** *321*, 385–388.
3. Du, X.; Skachko, I.; Barker, A.; Andrei, E. Y. Approaching Ballistic Transport in Suspended Graphene. *Nat. Nanotechnol.* **2008,** *3*, 491–495.
4. Morozov, S. V.; Novoselov, K. S.; Katsnelson, M. I.; Schedin, F.; Elias, D. C.; Jaszczak, J. A.; Geim, A. K. Giant Intrinsic Carrier Mobilities in Graphene and Its Bilayer. *Phys. Rev. Lett.* **2008,** *100*, 016602.
5. Novoselov, K. S.; Geim, A. K.; Morozov, S. V.; Jiang, D.; Katsnelson, M. I.; Grigorieva, I. V.; Dubonos, S. V.; Firsov, A. A. Two-Dimensional Gas of Massless Dirac Fermions in Graphene. *Nature* **2005,** *438*, 197–200.
6. Baladin, A. A.; Ghosh, S.; Bao, W.; Calizo, I.; Teweldebrhan, D.; Miao, F.; Lau, C. N. Superior Thermal Conductivity of Single-Layer Graphene. *Nano Lett.* **2008,** *8*, 902–907.
7. Chen, Z.; Lin, Y.-M.; Rooks, M. J.; Avouris, P. Graphene Nano-Ribbon Electronics. *Physica E* **2007,** *40*, 228–232.
8. Han, M. Y.; Özyilmaz, B.; Zhang, Y.; Kim, P. Energy Band-Gap Engineering of Graphene Nanoribbons. *Phys. Rev. Lett.* **2007,** *98*, 206805.
9. Wang, X.; Ouyang, Y.; Li, X.; Wang, H.; Guo, J.; Dai, H. Room-Temperature All-Semiconducting Sub-10-nm Graphene Nanoribbon Field-Effect Transistors. *Phys. Rev. Lett.* **2008,** *100*, 206803.
10. Kobayashi, Y.; Fukui, K.-I.; Enoki, T.; Kusakabe, K.; Kaburagi, Y. Observation of Zigzag and Armchair Edges of Graphite Using Scanning Tunneling Microscopy and Spectroscopy. *Phys. Rev. B* **2005,** *71*, 193406.
11. Zhao, P.; Choudhury, M.; Mohanram, K.; Guo, J. Computational Model of Edge Effects in Graphene Nanoribbon Transistors. *Nano Res.* **2008,** *1*, 395–402.
12. Cresti, A.; Roche, S. Range and Correlation Effects in Edge Disordered Graphene Nanoribbons. *New J. Phys.* **2009,** *11*, 095004.
13. Girit, Ç. Ö.; Meyer, J. C.; Erni, R.; Rossell, M. D.; Kisielowski, C.; Yang, L.; Park, C.-H.; Crommie, M. F.; Cohen, M. L.; Louie, S. G.; *et al.* Graphene at the Edge: Stability and Dynamics. *Science* **2009,** *323*, 1705–1708.
14. Warner, J. H.; Schäffel, F.; Rümmeli, M. H.; Büchner, B. Examining the Edges of Multi-Layer Graphene Sheets. *Chem. Mater.* **2009,** *21*, 2418–2421.
15. Liu, Z.; Suenaga, K.; Harris, P. J. F.; Iijima, S. Open and Closed Edges of Graphene Layers. *Phys. Rev. Lett.* **2009,** *102*, 015501.
16. Koskinen, P.; Malola, S.; Häkkinen, H. Evidence for Graphene Edges beyond Zigzag and Armchair. *Phys. Rev. B* **2009,** *80*, 073401.
17. Kobayashi, Y.; Fukui, K.-I.; Enoki, T.; Kusakabe, K. Edge State on Hydrogen-Terminated Graphite Edges Investigated by Scanning Tunneling Microscopy. *Phys. Rev. B* **2006,** *73*, 125415.
18. Ritter, K. A.; Lyding, J. W. The Influence of Edge Structure on the Electronic Properties of Graphene Quantum Dots and Nanoribbons. *Nat. Mater.* **2009,** *8*, 235–242.
19. Ye, M.; Cui, Y. T.; Nishimura, Y.; Yamada, Y.; Qiao, S.; Kimura, A.; Nakatake, M.; Namatame, H.; Taniguchi, M. Edge States of Epitaxially Grown Graphene on 4H-SiC(0001) Studied by Scanning Tunneling Microscopy. *Eur. Phys. J.* **2010,** *B 75*, 31–35.
20. Neubeck, S.; You, Y. M.; Ni, Z. H.; Blake, P.; Shen, Z. X.; Geim, A. K.; Novoselov, K. S. Direct Determination of the Crystallographic Orientation of Graphene Edges by Atomic Resolution Imaging. *Appl. Phys. Lett.* **2010,** *97*, 053110.
21. Casiraghi, C.; Hartschuh, A.; Qian, H.; Piscanec, S.; Georgi, C.; Fasoli, A.; Novoselov, K. S.; Basko, D. M.; Ferrari, A. C. Raman Spectroscopy of Graphene Edges. *Nano Lett.* **2009,** *9*, 1433–1441.
22. Gupta, A. K.; Russin, T. J.; Gutiérrez, H. R.; Eklund, P. C. Probing Graphene Edges *via* Raman Scattering. *ACS Nano* **2009,** *3*, 45–52.
23. Jiao, L.; Wang, X.; Diankov, G.; Wang, H.; Dai, H. Facile Synthesis of High-Quality Graphene Nanoribbons. *Nat. Nanotechnol.* **2010,** *5*, 321–325.
24. Li, X.; Wang, X.; Zhang, L.; Lee, S.; Dai, H. Chemically Derived, Ultrasmooth Graphene Nanoribbon Semiconductors. *Science* **2008,** *319*, 1229–1232.
25. Ci, L.; Xu, Z.; Wang, L.; Gao, W.; Ding, F.; Kelly, K. F.; Yakobson, B. I.; Ajayan, P. M. Controlled Nanocutting of Graphene. *Nano Res.* **2008,** *1*, 116–122.
26. Datta, S. S.; Strachan, D. R.; Khamis, S. M.; Johnson, A. T. C. Crystallographic Etching of Few-Layer Graphene. *Nano Lett.* **2008,** *8*, 1912–1915.
27. Tapasztó, L.; Dobrik, G.; Lambin, Ph.; Biró, L. P. Tailoring the Atomic Structure of Graphene Nanoribbons by Scanning

Tunnelling Microscope Lithography. *Nat. Nanotechnol.* **2008,** *3*, 397–401.
28. Wu, Z.-S.; Ren, W.; Gao, L.; Liu, B.; Zhao, J.; Cheng, H.-M. Efficient Synthesis of Graphene Nanoribbons Sonochemically Cut from Graphene Sheets. *Nano Res.* **2010,** *3*, 16–22.
29. Krauss, B.; Nemes-Incze, P.; Skakalova, V.; Biro, L. P.; von Klitzing, K.; Smet, J. H. Raman Scattering at Pure Graphene Zigzag Edges. *Nano Lett.* **2010,** *10*, 4544–4548.
30. Yang, X.; Dou, X.; Rouhanipour, A.; Zhi, L.; Räder, H. J.; Müllen, K. Two-Dimensional Graphene Nanoribbons. *J. Am. Chem. Soc.* **2008,** *130*, 4216–4217.
31. Cai, J.; Ruffieux, P.; Jaafar, R.; Bieri, M.; Braun, T.; Blankenburg, S.; Muoth, M.; Seitsonen, A. P.; Saleh, M.; Feng, X.; *et al.* Atomically Precise Bottom-Up Fabrication of Graphene Nanoribbons. *Nature* **2010,** *466*, 470–473.
32. Jiao, L.; Zhang, L.; Wang, X.; Diankov, G.; Dai, H. Narrow Graphene Nanoribbons from Carbon Nanotubes. *Nature* **2009,** *458*, 877–880.
33. Kosynkin, D. V.; Higginbotham, A. L.; Sinitskii, A.; Lomeda, J. R.; Dimiev, A.; Price, B. K.; Tour, J. M. Longitudinal Unzipping of Carbon Nanotubes To Form Graphene Nanoribbons. *Nature* **2009,** *458*, 872–876.
34. Cataldo, F.; Compagnini, G.; Patané, G.; Ursini, O.; Angelini, G.; Ribic, P. R.; Margaritondo, G.; Cricenti, A.; Palleschi, G.; Valentini, F. Graphene Nanoribbons Produced by the Oxidative Unzipping of Single-Wall Carbon Nanotubes. *Carbon* **2010,** *48*, 2596–2602.
35. Elías, A. L.; Botello-Méndez, A. R.; Meneses-Rodríguez, D.; Jehová González, V.; Ramírez-González, D.; Ci, L.; Muñoz-Sandoval, E.; Ajayan, P. M.; Terrones, H.; Terrones, M. Longitudinal Cutting of Pure and Doped Carbon Nanotubes To Form Graphitic Nanoribbons Using Metal Clusters as Nanoscalpels. *Nano Lett.* **2010,** *10*, 366–372.
36. Konishi, S.; Sugimoto, W.; Murakami, Y.; Takasu, Y. Catalytic Creation of Channels in the Surface Layers of Highly Oriented Pyrolytic Graphite by Cobalt Nanoparticles. *Carbon* **2006,** *44*, 2338–2340.
37. Campos, L. C.; Manfrinato, V. R.; Sanchez-Yamagishi, J. D.; Kong, J.; Jarillo-Herrero, P. Anisotropic Etching and Nanoribbon Formation in Single-Layer Graphene. *Nano Lett.* **2009,** *9*, 2600–2604.
38. Schäffel, F; Warner, J. H.; Bachmatiuk, A.; Rellinghaus, B.; Büchner, B.; Schultz, L.; Rümmeli, M. H. Shedding Light on the Crystallographic Etching of Multi-Layer Graphene at the Atomic Scale. *Nano Res.* **2009,** *2*, 695–705.
39. Gao, L.; Ren, W.; Liu, B.; Wu, Z.-S.; Jiang, C.; Cheng, H.-M. Crystallographic Tailoring of Graphene by Nonmetal SiO_x Nanoparticles. *J. Am. Chem. Soc.* **2009,** *131*, 13934–13936.
40. Malik, S.; Vijayaraghavan, A.; Erni, R.; Ariga, K.; Khalakhan, I.; Hill, J. P. High Purity Graphenes Prepared by a Chemical Intercalation Method. *Nanoscale* **2010,** *2*, 2139–2143.
41. Warner, J. H.; Rümmeli, M. H.; Gemming, T.; Büchner, B.; Briggs, G. A. D. Direct Imaging of Rotational Stacking Faults in Few Layer Graphene. *Nano Lett.* **2009,** *9*, 102–106.
42. Warner, J. H.; Rümmeli, M. H.; Ge, L.; Gemming, T.; Montanari, B.; Harrison, N. M.; Büchner, B.; Briggs, G. A. D. Structural Transformations in Graphene Studied with High Spatial and Temporal Resolution. *Nat. Nanotechnol.* **2009,** *4*, 500–504.
43. Dobrik, G.; Tapasztó, L.; Nemes-Incze, P.; Lambin, Ph.; Biró, L. P. Crystallographically Oriented High Resolution Lithography of Graphene Nanoribbons by STM Lithography. *Phys. Status Solidi B* **2010,** *247*, 896–902.
44. Hernandez, Y.; Nicolosi, V.; Lotya, M.; Blighe, F. M.; Sun, Z.; De, S.; McGovern, I. T.; Holland, B.; Byrne, M.; Gun'ko, Y. K.; *et al.* High-Yield Production of Graphene by Liquid-Phase Exfoliation of Graphite. *Nat. Nanotechnol.* **2008,** *3*, 563–568.
45. Schäffel, F.; Kramberger, C.; Rümmeli, M. H.; Grimm, D.; Mohn, E.; Gemming, T.; Pichler, T.; Rellinghaus, B.; Büchner, B.; Schultz, L. Nanoengineered Catalyst Particles as a Key for Tailor-Made Carbon Nanotubes. *Chem. Mater.* **2007,** *19*, 5006–5009.
46. Rümmeli, M. H.; Schäffel, F.; Bachmatiuk, A.; Adebimpe, D.; Trotter, G.; Börrnert, F.; Scott, A.; Coric, E.; Sparing, M.; Rellinghaus, B.; *et al.* Investigating the Outskirts of Fe and Co Catalyst Particles in Alumina-Supported Catalytic CVD Carbon Nanotube Growth. *ACS Nano* **2010,** *4*, 1146–1152.
47. Schäffel, F.; Warner, J. H.; Bachmatiuk, A.; Queitsch, U.; Rellinghaus, B.; Büchner, B.; Schultz, L.; Rümmeli, M. H. Tracking Down the Catalytic Hydrogenation of Multilayer Graphene. *Phys. Status Solidi C* **2010,** *7*, 2731–2734.
48. Smith, B. W.; Luzzi, D. E. Electron Irradiation Effects in Single Wall Carbon Nanotubes. *J. Appl. Phys.* **2001,** *90*, 3509–3515.
49. Warner, J. H; Schäffel, F.; Zhong, G.; Rümmeli, M. H.; Büchner, B.; Robertson, J.; Briggs, G. A. D. Investigating the Diameter-Dependent Stability of Single-Walled Carbon Nanotubes. *ACS Nano* **2009,** *3*, 1557–1563.